myelin regeneration in adult CNS, Nogo, myelin associated glycoprotein (MAG) and oligodendrocyte-myelin glycoprotein (OMgp) (Fournier et al., 2001; Wang et al., 2002a; Steinbach et al., 2011). Although Nogo-A expression was found in oligodendrocytes, its receptor NgR1 is primarily expressed by different types of mature neurons (Wang et al., 2002b; Fischer et al., 2004). But, both Nogo-A and NgR1 have been found in progenitors during development (Mingorance et al., 2004), neurosphere cells (Mathis et al., 2010), astrocytes (Wang et al., 2002b) and adult neural stem cells in subventricular zone (SVZ) (Ronaldo et al., 2012), suggesting additional functions for this pathway like neurosphere cell proliferation (Li et al., 2011) and differentiation (Wang and Zhu, 2008).

Multiple sclerosis (MS) is the most frequent chronic neurological disease of young adults (Noseworthy et al., 2000). Immune-mediated events are assumed to cause myelin loss and oligodendrocytes death, leading later to axonal injury (Nait-Oumesmar et al., 2007). MS affects optic chiasm and nerves in more than 70% of the patients (Guazzo, 2005). Demyelinated plaques can be remyelinated, although this remyelination is not adequate to overcome disease progression (Nait-Oumesmar et al., 2007). Different reasons might cause remylination impairment in demyelination lesion such as hormonal changes, stress oxidative and excitotoxicity (Mohajeri et al., 2015; Sherafat et al., 2011).

The SVZ of the lateral ventricles is one of the largest germinative areas and source of neural stem cells (NSCs) of the adult brain (Alvarez-Palazuelos et al., 2011). These cells can react to a range of insults including seizure, ischemia or demyelination by proliferation and migration into the adjacent injuries and differentiation into neuron or myelin- forming cells (Picard-Riera et al., 2004). Proliferation and neurogenesis increased the SVZ of patients with alzheimer (Jin et al., 2004), huntigton (Curtis et al., 2003), epilepsy (Crespel et al., 2005) and MS (Nait-Oumesmar et al., 2007). In addition, these cells also proliferate, migrate and differentiate into astrocyte and oligodendrocyte in response to lysolecithin-induced demyelination of the corpus callosum and optic chiasm (Picard-Riera et al., 2002; Mozafari et al., 2011; Sherafat et al., 2012). Previous studies have shown that different approaches in animal models of MS like basic fibroblast growth factor or valproic acid treatment enhanced SVZ stem cells proliferation and recruitment to the lesion sites (Dehghan et al., 2012, Pazhoohan et al., 2014). NgR is expressed in SVZ NSCs and progenitors and it can affect their proliferation potential in different conditions (Ronaldo et al., 2012). Nonetheless, little is known about the role of NgR in SVZ niche response to demyelination insult far from lateral ventricles and it is still uncertain.

Regarding the vulnerability of optic chiasm in MS disease and its anatomical distance from SVZ niche we used this area for local model of demyelination (Mozafari et al., 2011; Pourabdolhossein et al. 2011). The main objective was to study the effect of NgR inhibition on SVZ niche behavior in demyelination context. Here we provide histological and immonohistochemical evidences that NgR negatively regulated proliferation and differentiation of SVZ progenitor cells in demyelination context.

Materials and methods

Animals

All animal studies were conducted according to the principles and procedures described in Guidelines for care and use of experimental animals and were approved by Tarbiat Modares University-Ethics Committee for Research on Animals. Eight week-old (25-30g) males C57BL/6 were purchased from Razi institute, Iran and JANVIER (Le Genest St Isle, France). Animals were kept (five per cage) under 12 h light/dark cycles with controlled temperature (22± 2°C) and food and water were available ad libitum. The number of animals used for each group was eight (n=8).

Demyelination procedure

Animals were deeply anesthetized with intraperitoneal (ip) injection of ketamin (70mg/kg, Alfasan) and xylazine (10mg/kg, Alfasan) dissolved in 0.9% strile saline. Demyelination was induced by stereotaxic injection of 1µl of solution of 1% lysolecithin (LPC; sigma, stlouis, USA) in 0.9% NaCl (Mozafari et al., 2010). Control animals were injected with equal volume of sterile saline. Mice were positioned in a stereotaxic device (steolting, USA) in a skull flat situation. The LPC (1µl 1% solution) was injected into the optic chiasm, using the stereotaxic coordinates of 3.9 mm anterior to the lambda, 5.75 mm deep from dura surface and zero laterality

(Paxinos and Franklin, 2004). The needle was kept in place for 5 min to equilibrate tissue and injected solution and avoided the possible reflux through the needle tract. Stereotaxic injection of 2% Evan's blue into optic chiasm coordinates was done to assess the injection site (data not shown).

Interventions

We used validated siRNA against NgR1 (Rtn4r,4 different sequences, cat no: SI02722888, SI02699186, SI02748333, SI02678249) and pGL2 (for control group) from Qiagen. We diluted siRNA (24 pmol per animal) in glucose (5%) and mixed with monocationic lipid (IC10, Polyplus-transfection) at a ratio of 15 monocationic lipid nitrogens per RNA phosphate as described before (Remaud et al., 2013; Pourabdolhossein et al., 2014). Complexes prepared at room temperature are stable for two hours after preparation. For intracerebroventricular (ICV) administration of siRNAs, animals were cannulated unilaterally in the right lateral ventricle (3.6 mm anterior to lambda, 1.1 mm lateral and 2.2 mm deep from the dura surface) (Paxinos and Franklin, 2004). To knockdown NgR, animals received daily ICV injection of siRNA (24 pmol/2 µl) from permanent cannula. Control groups received same volume of saline.

Real time PCR

The border of lateral ventricle of adult mice was dissected, snap-frozen in liquid nitrogen and stored at -80°C until processed. The total RNA was extracted based on the protocol provided with the RNAble reagent (Eurobio, Les Ulis, France), measured RNA concentration and stored in Tris 10 mM/EDTA 0.1mM (pH 7.4) at -80°C. To quantify mRNAs 1µg of total RNA was reverse-transcribed using High capacity cDNA Reverse Transcription kit (Applied Biosystems, Courtaboeuf, France). In parallel we did control reactions without reverse transcriptase. Primers for the detection of NgR (Taqman gene expression assays, references: Mm00710554-m1) and control assay GAPDH (Mm99999915-g1) were purchased from Applied Biosystems. Direct detection of the PCR product was monitored by measuring the increase in fluorescence generated by the TaqMan probe (NgR, GAPDH) as previously described (Decherf et al., 2010).

Cell tracing

Bromodeoxyuridine (5-bromo-2-deoxyuridine, BrdU) is incorporated into DNA during S phase of the cell cycle; therefore it is an appropriate marker of newly divided cell. To trace stem cell pools in SVZ after demyelination and treatment with siNgR we used seven injections of Brdu (sigma, USA) at intervals of 2 h (70 mg/kg each, ip) 24 h prior to demyelination for each animal and they were euthanized 3, 7 and 14 days after demyelination (Picard-Riera et al., 2002). The labeled cells are restricted to the SVZ in controls in this tracing protocol; therefore, detection of labeled cells after demyelination in structures other than the SVZ and Rostral Migratory Stream (RMS) is implied to originate from SVZ or RMS (Decker et al., 2002; Picard-Riera et al., 2002; Nait-Oumesmar et al., 1999).

Tissue processing

We deeply anesthetized mice with high dose of ketamin/xylazine on 3, 7 and 14 days post lesion and perfused them intracardially with a fresh 0.1 M phosphate buffered saline (PBS) and then with a solution of 4% paraformaldehyde in PBS. Brains were excised and post-fixed overnight into the same fixative solution at 4°C. For paraffin embedding, brains were first dehydrated in a series of alcohols with increasing concentrations, cleared by incubation in xylene (2×45 min) and finally embedded in paraffin for 2×6 hours and blocked. The 21 serial coronal sections (6µm thickness) with 48µm intervals (+100-700µm) from bregma were obtained using a rotary microtome (lieca, Austria).

For cryosection, brains were removed and kept in the same fixative for 6 h and stored overnight at 4°C in a 0.1 M PBS solution containing 20% sucrose, then embedded in Cryomatrix and stored at -80°C. Coronal sections (12µm) were obtained using a Cryostat (Leica, Rueil-mal maison, France) and collected on superfrost plus slides (Thermo Scientific). Coronal serial sections with 120µm intervals (+20-800µm from bregma) were analyzed.

Luxol fast blue (LFB) staining

LFB staining was performed to assess demyelination and remyelination processes in optic chiasm as previously described (Pourabdolhossein et al., 2011; Mozafari et al., 2011). In brief, sections were stained with 0.1% LFB (British drug house, UK) solution at 60°C for 3 h. Adequate contrast was obtained by

rapid immersion of slides in 0.05% lithium carbonate and 70% ethanol. After washing with tap water, sections were counterstained with 0.1% cresyl fast violet (merck, Germany) for 5 minute. Sections were washed in distilled water again and dehydrated in a graded series of alcohols, then cleared in xylene and cover slipped. Images were captured with DP-27 camera. The extent of demyelination, as the ratio of lesion size per total area, was assessed by Image J software according to the method described in detail elsewhere (Chitnis et al., 2007). Data obtained from each group was averaged for all 21 point of each animal (n=3).

Immunohistochemistry

The proliferating cells in SVZ were identified using a rat anti-Brdu antibody (1/500; AbD serotoles, MCA2060) and co-labeled with rabbit anti Olig2 antibody (1/500, Millipore, AB9610), rabbit anti GFAP (1/500, Dako, Z0334) and mouse anti PSA-NCAM (1/400, AbCys, AbC0019) to characterize Brdu+ cells. Cryosections were rehydrated in 0.1 M PBS three times for 5 min and incubated 1 h with blocking solution containing 10% normal goat serum (Vector Laboratories, France 501000) and bovine serum albumin 2 mg/ml (Vector Laboratories- sp50-50) and 0.3% triton X100 (sigma, USA) in PBS. Slides were incubated overnight at 4°C with primary antibodies diluted in blocking solution and cover slipped. Then, slides were rinsed three times for 10 min with PBS and incubated with secondary antibody (Alexa Flour 488nm, Invitrogen) for 1 h at room temperature (RT). For double labeling with BrdU, sections were washed three times in PBS for 10 min and incubated in HCl 2N for 30 min at 37°C, after two washes 5 min in borate buffer (pH: 8.4) and PBS, sections were incubated with the same blocking solution and incubated overnight at 4°C with the anti Brdu antibody diluted in blocking solution. After washing, sections were incubated with secondary antibody (1/500, invitrogen, A11007) for 1 h at RT. After several washes with PBS, brain sections were mounted in antifade reagent with DAPI (P3693, Invitrogen) and analyzed under fluorescent microscopy on an Olympus AX70 microscope and camera Olympus DP50. For cell counting in the SVZ 12µm sections were used. The number of total BrdU+cells and Brdu+/ Olig2+, Brdu+/GFAP+ or Brdu+/PSA-NCAM+ positive cells was averaged from three different levels 120µm apart and three consecutive sections per level. Data obtained from each group was averaged from nine sections (each brain). Data were expressed in number of cells per field and are deduced from three mice per experimental group.

Statistical analysis

The result is expressed as mean±SEM. Data were analyzed by two-way analysis of variance (ANOVA) followed by Bonferroni post-tests with Graph pad PRISM software (Graph pad software, Inc, San Diego. CA). Data were determined to be significant when $P<0.05$.

Results

Nogo receptor successfully knockdown using siNgR *in vivo*

The putative role of NgR in SVZ progenitors proliferation and differentiation was studied by siRNA technology. We used siRNA/IC10 which is the first generation of lipid based siRNA vectors as previously described (Remaud et al., 2013; Pourabdolhossein et al., 2014). It was confirmed that IC10 vectorizes siRNA into cells expressing NSC markers in the adult SVZ (Remaud et al., 2013). To knockdown NgR, a validated siRNA targeting NgR1 was injected stereotaxically into the lateral ventricle of adult mice brain. We carefully sampled the area of lateral ventricles and SVZ 24, 48 and 72 h after siRNA injection and RNA was extracted for qPCR analysis. We observed a significant ($P<0.001$) decrease (0.40 fold change) in NgR mRNA expression 24 h after the injection, in NgR-siRNA group when compared to control-siRNA (Fig. 1). In later time points we did not observe significant differences between siNgR and siControl groups. Our results show that siRNA mediated knockdown of NgR was efficient and transient. We used daily intraventricular injection of 24 pmol siNgR/IC10, to knockdown NgR during the process of the LPC demyelination/ remyelination (2 weeks).

NgR inhibition reduce demyelination extention in demyelinated optic chiasm of mice

To investigate the role of NgR on SVZ reactivation in a demyelinating context, we induced a local demyelination in the optic chiasm using LPC injection

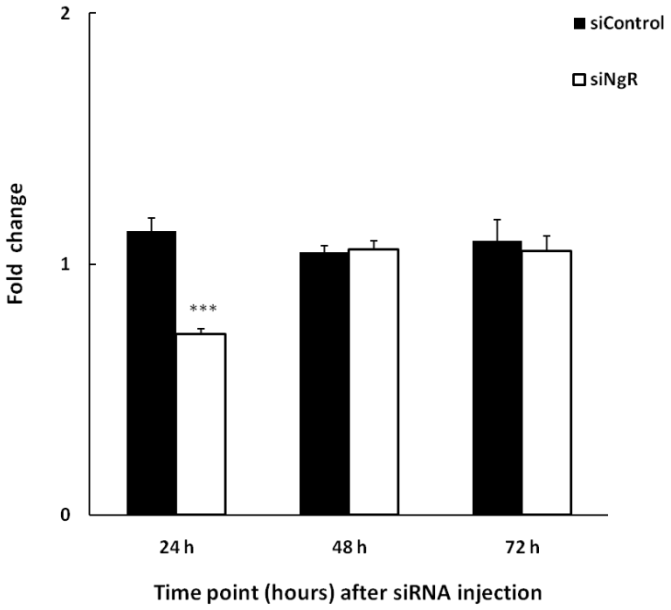

Fig.1. NgR knockdown mediated by siRNA. qPCR of lateral ventricle samples show levels of NgR expression at 24, 48 and 72 hrs after single siRNA injection. We normalized our Gene expression with GAPDH. Data are pooled from three independent experiments providing similar results (total number of mice for each data point = 6). Graph shows fold changes in NgR mRNA using qPCR analysis. Statistical analysis used one-way ANOVA and Bonferroni's post -test. NgR gene expression was decreased significantly 24 h after siNgR injection compared to siControl, the asterisk indicates that the difference between the pairs denoted are significant at the confidence levels $^{***}P<0.001$.

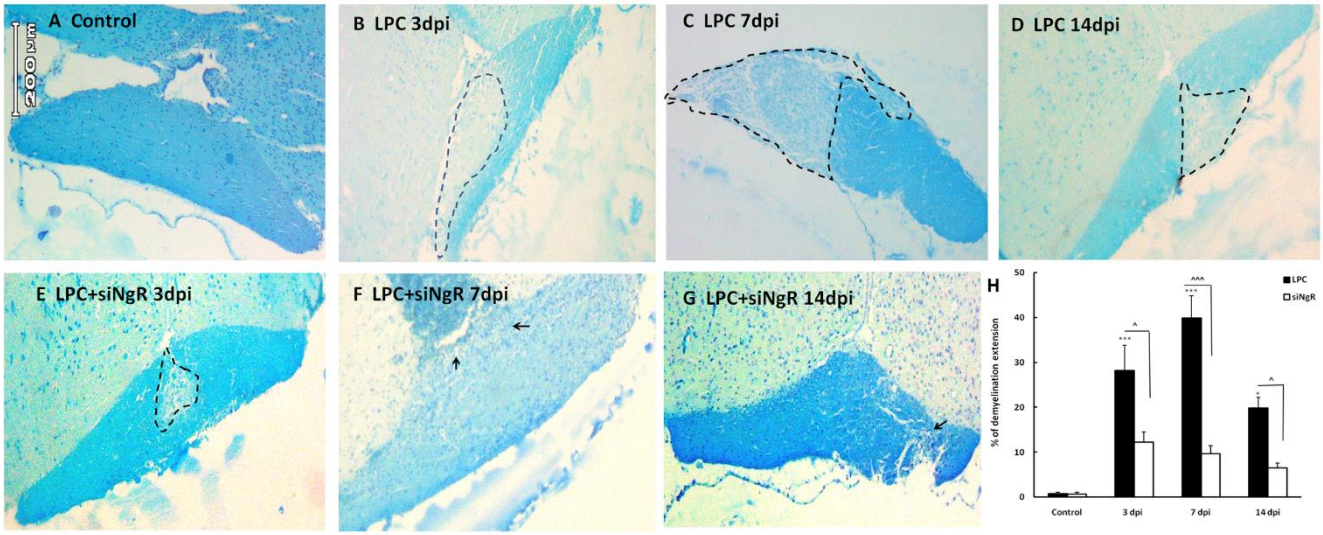

Fig.2. NgR knock down decreased demyelination extention. Coronal sections of adult mouse brains (6mm) treated with saline, LPC and LPC+siNgR were stained with Luxol fast blue and cresyl fast violet (A) Saline-treated chiasm at 7 days post injection (dpi), no visible demyelination is seen 7 days after a single injection of saline (control). (B-D) Demyelination at optic chiasm of LPC-treated animals at 3, 7 and 14 dpi, respectively. (E-G) Demyelination at optic chiasm of LPC+siNgR treated animals at 3, 7 and 14 dpi, respectively. (H) The extent of demyelination in different groups presented as percent of total area and quantitatively analyzed. Statistical analysis used two-way ANOVA and Bonferroni's post -test. Treatment with siRNA had a significant effect on the myelin repair. In LPC treated-animals significant demyelination is seen at 3, 7 and 14 dpi compared to control ($^{***}P<0.001$, $^{*}P<0.05$). Between groups, there was a significant reduction of demyelination in LPC+siNgR 3 dpi compared to LPC 3 dpi ($^{\wedge}P<0.05$) and in LPC+siNgR 7 dpi compared to LPC 7 dpi ($^{\wedge\wedge\wedge}P<0.001$). Data are expressed in mean±SEM Scale Bar is 200 µm in all pictures and dashed line indicates lesion area (n≥3).

as previously described (Dehghan et al., 2012; Mozafari et al, 2011, Pourabdolhossein et al., 2011). Dye study was done to show a confined injection site into the chiasm without extra distribution into other structures or surrounding cerebrospinal fluid (data not shown). We used LFB staining to confirm our model and evaluate the demyeliation extension in different groups (Fig. 2). Demyelination extent was calculated

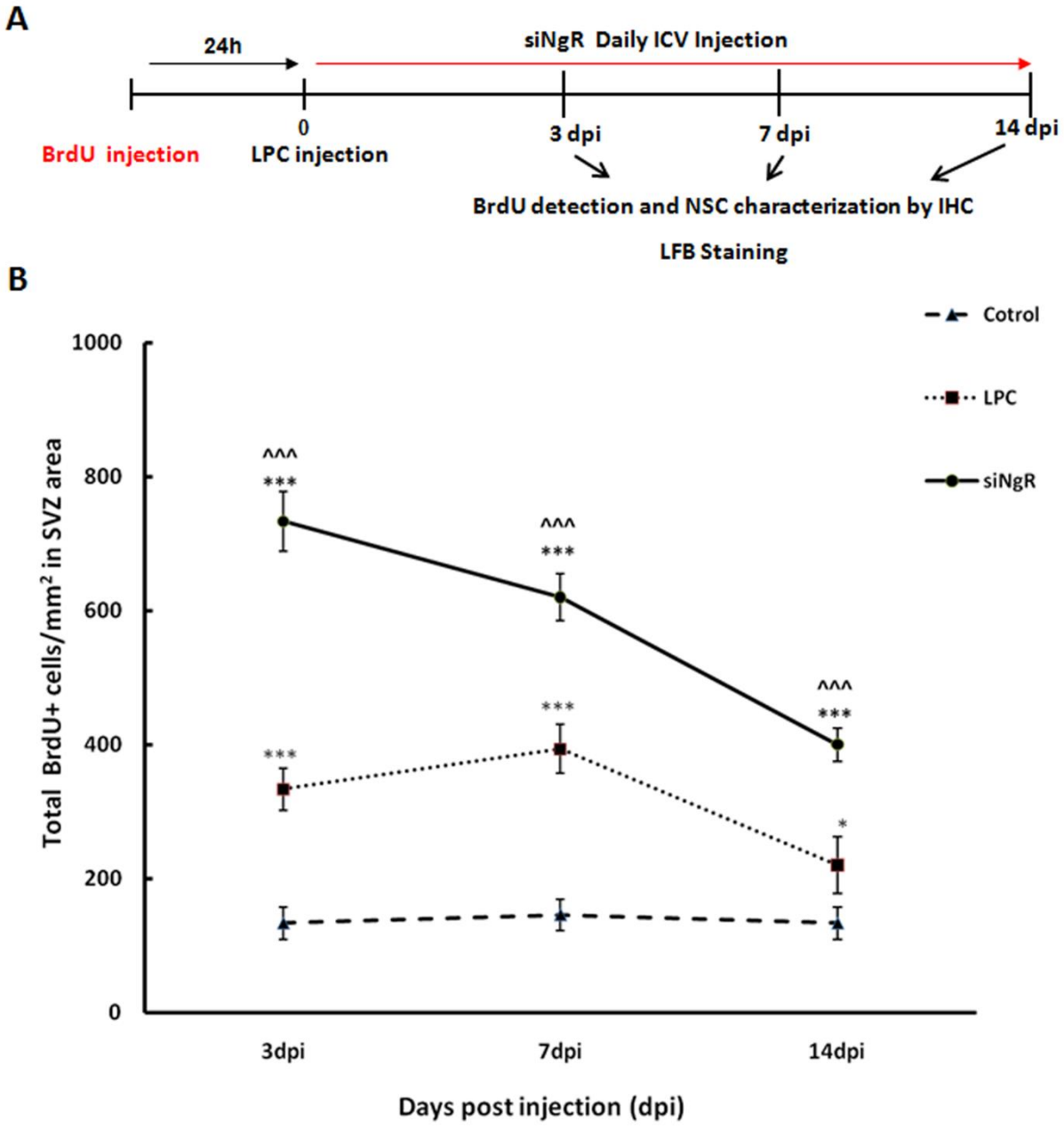

Fig.3. SVZ progenitor cell activation in response to LPC-induced lesions in optic chiasm is greater following NgR inhibition. (A) A chronological figure of experimental procedure shows the time of BrdU and LPC injection and daily treatment with siNgR and sampling in different groups. Mice received seven injections of Brdu at intervals of 2 h, 24 h prior to demyelination, and were sacrificed 3, 7 or 14 days after LPC injection for VEP recording, LFB staining, characterization of NSC by IHC. (B) Total BrdU+ cells per field are quantified and averaged from the counts of nine sections in each animal (n=3). Statistical analysis of the differences between total numbers of BrdU+ cells in the SVZ of all groups were done by two-way ANOVA followed by Bonferroni's post-test. Differences between groups were significant at all time points (P<0.001). Post-test showed that the total number of BrdU+ cells in LPC treated animals in 3 , 7 and 14 dpi were significantly different compared to control (P<0.001, P<0.05; respectively). In LPC+siNgR treated animals total number of BrdU+ cells at 3 , 7 and 14 dpi in the SVZ was considerably increased compared to control ($^{***}P$<0.001). NgR inhibition enhance the number of BrdU+ cells in SVZ compared to LPC groups and this change was significant between siNgR 3 dpi , LPC 3 dpi and siNgR 7 dpi , LPC 7 dpi and siNgR 14 dpi , LPC 14dpi ($^{\wedge\wedge\wedge}P$<0.001). Data are expressed as mean±SEM.

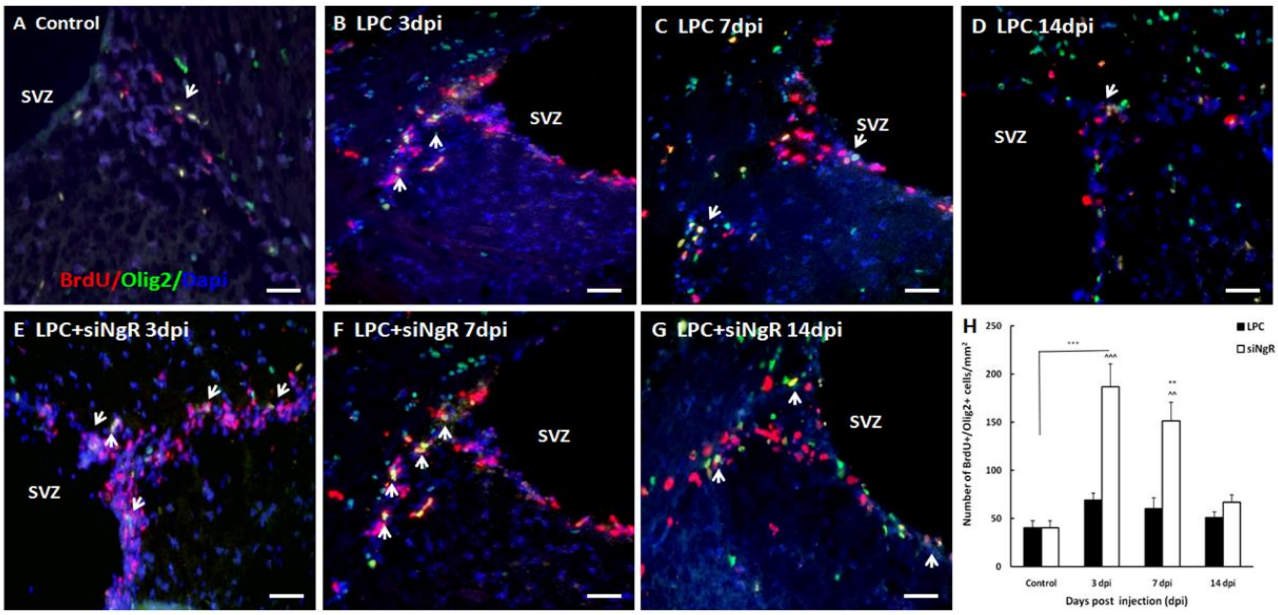

Fig.4. Increased BrdU+/Olig2+cell numbers in SVZ following NgR inhibition. Double immunohistochemistry (IHC) of BrdU (red) and Olig2 (green)-labeled cells was done on coronal section of lateral ventricles in different groups.(A) Low number of BrdU+/Olig2+ cells in SVZ of saline-treated animals at 7 dpi (control). (B–D) BrdU+/Olig2+cells in SVZ of LPC-treated animals at 3 (B), 7 (C) and 14 (D) dpi. (E–G) Cell expansion in SVZ of LPC+siNgR treated animals at 3 (E), 7 (F) and 14 (G) dpi. Arrows indicate double-labeled cells. (H) BrdU+/Olig2+cells per field are averaged from the counts of nine sections of each SVZ. Statistical analysis used two-way ANOVA with Bonferroni's post-test. In LPC treated groups the number of BrdU+/Olig2+cells was increased over the time but changes were not significant compared to control. In LPC+siNgR treated animals, the number of BrdU+/Olig2+cells at 3 and 7 dpi in the SVZ was increased compared to control ($^{***}P$ <0.001,$^{**}P$<0.01; respectively). Between groups significant changes exist at 3 dpi ($^{\wedge\wedge\wedge}P$ <0.001) and 7 dpi ($^{\wedge\wedge}P$ <0.01). Data are expressed as mean±SEM, n = 3, Bars: 50mm.

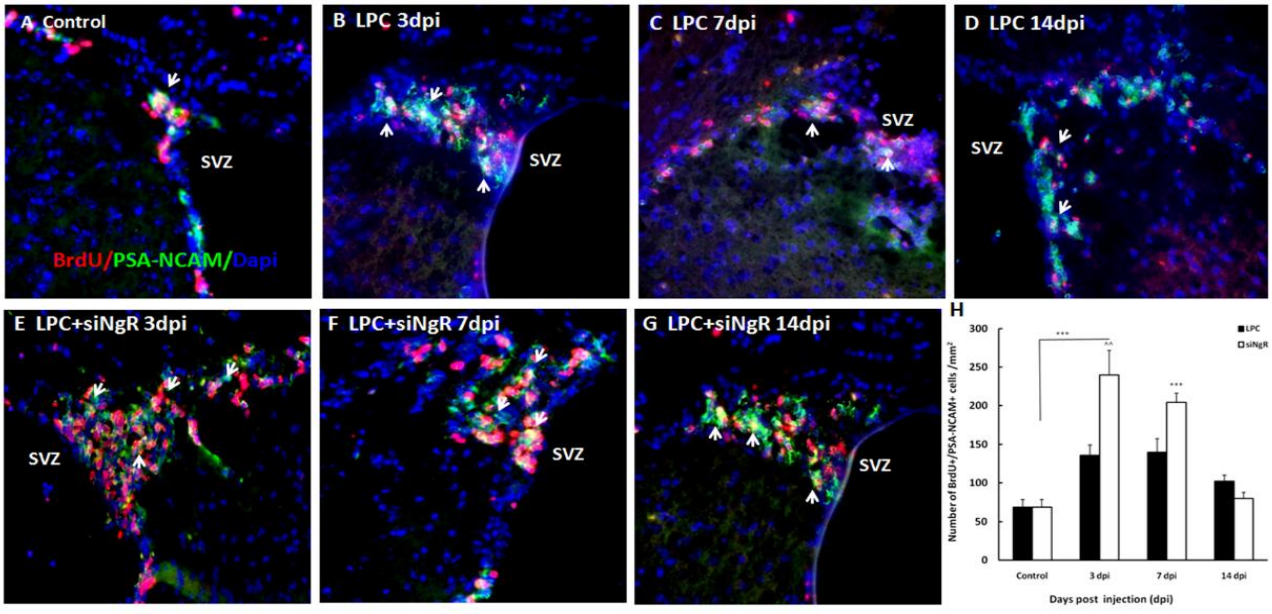

Fig.5. Increased BrdU+/PSA-NCAM+ cell numbers in SVZ following NgR inhibition. Double labeling of BrdU (red) with PSA-NCAM (green) was done in coronal sections of lateral ventricle area in different groups. (A) The number of BrdU+/PSA-NCAM+ cells in SVZ of control group. (B–D) BrdU+/PSA-NCAM+cells in SVZ of LPC-treated animals at 3 (B), 7 (C) and 14 (D) dpi. (E–G) Cell expansion in SVZ of LPC+siNgR treated animals at 3 (E), 7 (F) and 14 (G) dpi. Arrows indicate double-labeled cells. (H) Histograms show quantification of double marker positive cells in different groups. In LPC treated groups there is no significant changes of BrdU+/PSA-NCAM+ cell number compared to control. The number of BrdU+/PSA-NCAM+cells in LPC+siNgR treated animals, at 3 and 7 dpi in the SVZ was considerably increased compared to control ($^{***}P$ <0.001). There are significant changes exist at 3 dpi ($^{\wedge\wedge}P$ <0.01) between groups. Data are expressed as mean±SEM, n = 3, Bars: 50mm.

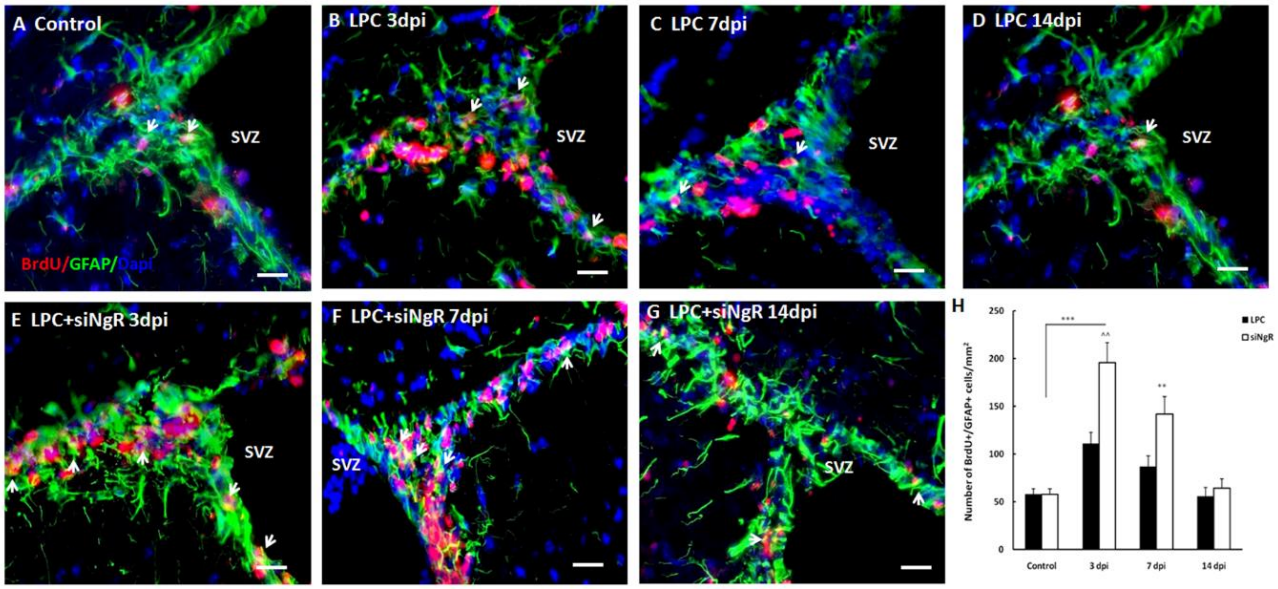

Fig.6. The numbers of BrdU+/GFAP+cells in SVZ increased following NgR inhibition. Immunofluorescent images of SVZ with double labeling of BrdU (red) and GFAP (green) in different groups. (A) The number of BrdU+/GFAP+ cells in SVZ of control group. (B-D) The number of BrdU+/GFAP+cells in SVZ of LPC-treated animals at 3 (B), 7 (C) and 14 (D) dpi. (E–G) SVZ images of LPC+siNgR treated animals at 3 (D), 7 (E) and 14 (F) dpi shows reactivation of SVZ is significant at day 3. Arrows indicate doublelabeled cells. (H) BrdU+/GFAP+cells per field are quantified and averaged from the counts of nine sections. Statistical analysis of the differences between numbers of BrdU+/GFAP+cells in the SVZ of all groups was done by two-way ANOVA followed by Bonferroni's post-test. Differences between groups were significant at day 3 (P <0.001). Post-test showed that the number of BrdU+/GFAP+cells in LPC treated animals in different time points were not significantly different compared to Control. In LPC+siNgR treated animals the number of BrdU+/GFAP+cells at 3 and 7 dpi in the SVZ was considerably increased compared to control ($^{***}P$ <0.001,** P <0.01; respectively). NgR inhibition enhance the number of BrdU+/GFAP+cells in SVZ compared to LPC groups and this change was significant between siNgR 3 dpi and LPC 3 dpi ($^{\wedge\wedge}P$ <0.001). Data are expressed as mean±SEM, n= 3, Bars: 50mm.

as percentage of total area of optic chiasm. No demyelination was detected in the optic chiasm of saline-treated animals (Fig. 2A). The demyelination extension significantly increased as early as day 3 in LPC treated animals and was maximal at 7 days post injection (dpi) compared to controls (P<0.001, Fig. 2 B-C). In LPC treated groups after 14 days, the extent of demyelination was reduced but compared to the control was significant (P<0.05, Fig. 2D). In siNgR treated animals, the demyelination area was considerably reduced at day 3, 7 and 14 post injections compared to the same days of LPC groups (P<0.05, P< 0.001 and P<0.05 respectively, Figs. 2E-H). siNgR treatment reduced demyelination extension probably through recruitment of endogenous stem cells and enhancement of myelin repair (p ourabdolhossein et al., 2014).

NgR inhibition potentiated SVZ stem cell expansion after LPC-induced demyelination in optic chiasm

To determine whether progenitor and stem cells, located in the SVZ, are able to respond to demyelination, and how NgR inhibition can affect their behavior, coronal brain sections of mice in different groups were double immune-labeled with the anti-BrdU, anti-Olig2, PSA-NCAM and GFAP antibodies to specifically characterize progenitor cells. We used the cell tracing protocol as previously described and BrdU was injected 24h prior to demyelination induction (Pourabdolhossein et al., 2014, Karnezis et al., 2004).

We analyzed total BrdU+ cell number in SVZ area of the mice brain and found that the number of BrdU+ cells considerably increased in all time points of LPC-treated animal compared to control ($^{***}P$<0.001, Fig. 3). However, in siNgR+LPC treated animals the number of total BrdU+ cells showed a two-fold increase compared to LPC groups at 3, 7 and 14 dpi ($^{\wedge\wedge\wedge}P$<0.001, Fig. 3). We can conclude that although LPC-induced demyelination in optic chiasm can activate and expand SVZ area, NgR inhibition can

robustly increase SVZ stem cell proliferation.

SVZ stem cells differentiation is increased in response to NgR knockdown

We previously showed that NgR inhibition in demyelination context activated proliferation of local progenitor in the third ventricle and optic chiasm (Pourabdolhossein et al., 2014). In this study we observed that inhibition of NgR resulted in a greater response from the SVZ of lateral ventricle following LPC lesion in the mouse optic chiasm. To characterize proliferating cell types in SVZ, BrdU+cells were co-labeled with the antibodies against Olig2 (oligodendrocyte lineage), PSA-NCAM (neuroblast lineage) and GFAP (astrocytes lineage).

The analysis showed that the number of BrdU+/Olig2+ cells residing in SVZ area was increased at day 3 and 7 dpi in LPC treated mice but changes were not significant between groups (Fig. 4 A-D). However in siNgR+LPC treated animals at 3 and 7 dpi the number of BrdU+/Olig2+ cells considerably increased compared to the control and LPC groups at 3 and 7 dpi respectively ($^{***}P$<0.001, $^{**}P$<0.01, $^{\wedge\wedge\wedge}P$<0.001, $^{\wedge\wedge}P$<0.01, Fig. 4 E-H). In LPC alone the number of BrdU+/PSA-NCAM+ cells was not notably increased compared to the control, while the number of those cells in SVZ of siNgR treated group at 3 and 7 dpi drastically increased compared to control ($^{***}P$<0.001) and only at day 3 was significant compared to LPC-treated groups ($^{\wedge\wedge}P$<0.01, Fig. 5A-H). Numbers of BrdU+/GFAP+cells was not significantly modified in LPC treated animals compared to controls, whereas in siNgR treated animals BrdU+/GFAP+cells significantly increased in the lateral ventricle SVZ at 3 and 7 dpi compared to controls ($^{***}P$<0.001, $^{**}P$<0.01, Fig. 6 A–H). Number of BrdU+/GFAP+cells was significantly increased at day 3 in siNgR treated group compared to LPC treated animals ($^{\wedge\wedge}P$<0.01, Fig. 6 B, E and H).

Taken together, our results suggest that dividing cells in SVZ area differentiated to different cell types in response to LPC insults and NgR inhibition enhances differentiation potential of these cells at this neurogenic region.

Discussion

In this study we clarified that local demyelination of optic chiasm can partially activate proliferation and mobilization of progenitor cells from SVZ of lateral ventricles (Pourabdolhossein et al., 2014, Mozafari et al., 2011). We also provide evidence that NgR signaling restricts SVZ progenitor cells proliferation and differentiation to different cell types in demyelination context. In addition, we show that NgR knockdown reduced demyelination extension in optic chiasm.

To locally inhibit NgR, we injected siRNA against NgR into lateral ventricle of adult mouse and evaluated the efficiency of NgR blockade by real time PCR for NgR mRNA in the tissue isolated from lateral ventricle. Real time PCR quantification demonstrated that the siRNA inhibits NgR gene expression by up to 40%, 24 hours after *in vivo* injection. Therefore, we applied daily injection of siRNAs against NgR (siNgR) through permanent cannula following LPC-induced demyelination localized in the optic chiasm. Our results show that siNgR treatment over 14 days progressively and significantly reduced demyelination extension in optic chiasm.

Interaction of myelin inhibitory proteins (MAG, OMgp and Nogo) with NgR is the major candidate affecting axonal outgrowth and regeneration in the adult CNS (Fournier et al., 2001). A bunch of studies have used different blocking strategies to assess the role of NgR on axonal repair, in the animal models of CNS damage such as spinal cord injury (Harvey et al., 2009), stroke (Wang et al., 2010) and demyelination models of MS (Petratos et al., 2012; Yang et al., 2010; Karnezis et al., 2004). It is well documented that inhibition of NgR can enhance axonal repair during injury. NgR is expressed in cells other than neurons including NSCs (Mathis et al., 2010; Wang et al., 2008a; Wang et al., 2008b), oligodendrocyte precursor cells (Huang et al., 2012), astrocytes (Satoh et al., 2005) and schwann cells (Fry et al., 2007), suggesting additional function for NgR pathway in physiology and pathological condition.

Our previous studies showed that progenitor cells in the third ventricle surroundings could be reactivated by adjacent chiasm demyelination (Mozafari et al., 2011) and NgR blockade enhanced their migration potential to the lesion site (Pourabdolhossein et al., 2014). Also NgR blockade *in vitro* increases the total cover distance and maximum speed of migration of precursors in neurosphere (Su et al., 2007). In addition, it has been reported that Nogo-A and NgR1 regulated adult NSCs homeostatic function in SVZ

and neuroblast migration (Ronaldo et al., 2012). However, the molecular pathway of NgR signaling in SVZ progenitor's reaction in demyelination condition is still undefined. To investigate the effect of NgR inhibition on SVZ cells *in vivo*, we pre-labeled the proliferating cells by BrdU before induction of LPC lesion in adult mouse optic chiasm. Our results reveal that the total number of BrdU+cells was significantly increased in SVZ of demyelinated mice treated with siNgR at 3 and 7 dpi when compared to LPC and saline treated groups. This data proves that NgR negatively regulated NSCs proliferation in SVZ. Li and coworkers (2011) have shown that NgR inhibited the proliferation of neural progenitor cells *in vitro* via notch pathway. It is also reported that NgR signaling stimulates NSC survival and proliferation *in vitro* (Ramasamy et al., 2014).

In addition to demyelination, oligodendrocyte cell death and neuronal loss are also important pathological characteristics of MS (Nait-Oumesmar et al., 2007). Oligodendroglial precursor cells (OPCs) are considered the main source for differentiating into mature myelinating oligodendrocytes (Kremer et al., 2016). Thus, promoting differentiation potential of OPCs could be a target for repair in MS. Groups of studies demonstrated that myelin inhibitory proteins through NgR mediates inhibition of OPC differentiation and impairs CNS remyelination (Baer et al., 2009; Kotter et al., 2006). Characterization of SVZ proliferating cell types revealed that NgR inhibition increases BrdU+/Olig2+, BrdU+/GFAP+ and BrdU+/PSA-NCAM+ populations in SVZ compared to LPC and control animals. Interestingly, the number of BrdU+/Olig2+ cells considerably enhanced at 3 and 7 dpi in siNgR treated animal compared to LPC and control groups while the number of other two cell types persevered higher than control only at 3 dpi. This data fits with that of Chong et al. (2012) who showed that mice lacking Nogo-A (NogoA-/-) have increased myelinogenic potential of oligodendrocytes. The inhibitory effect of Nogo-A on OPCs differentiation *in vitro* has also been shown by Syed and colleagues (2008). However, Wang and others reported that exposure of neural stem cells with Nogo-66 promotes glial but inhibits neuronal differentiation *in vitro* (Wang et al., 2008b). The current study demonstrates that NgR inhibition significantly increased the number of SVZ BrdU+/PSA-NCAM+ cells (neuroblast marker) in early time points of the disease compared to LPC group. Our quantification data showed that the number of all three cell types increased in siNgR treated groups compared to LPC group at 3 dpi and only BrdU+/Olig2+ cells persisted high up to 7 dpi. So we suggest that the nature of lesion causes persevered differentiation of SVZ proliferating cells to OPCs in longer time. Our previous data showed that NgR inhibition functionally increases myelin repair, as evidenced by an enhancement in progenitor cell migration to the lesion site and this was concurrent with recovery in visual evoked potential features (pourabdolhossein et al. 2014). Recent data showed that the number of all BrdU+/Olig2+, GFAP+ and PSA-NCAM+ cells in SVZ notably decreased at 14 dpi in LPC+siNgR groups compared to day 3. This reduction at 14 dpi suggests that progenitor cells located in SVZ were mobilized and migrated in response to the LPC-induced demyelination in the optic chiasm when NgR was blocked (pourabdolhossein et al., 2014). Several studies showed that SVZ reactivation and mobilization of proliferating cells in response to demyelination insults (Pourabdolhossein et al., 2017; Nait-Oumesmar et al., 2007; Picard-Riera et al., 2004); nevertheless, to our knowledge, the current data are the first to show that NgR blockade enhanced proliferation and differentiation potential of SVZ cells in demyelination context.

Conclusion

In the present study, we observed a reduced demyelination area in all time points in the optic chiasm of siNgR treated groups. We conclude that: first, inhibition of NgR could enhance proliferation and differentiation potential of SVZ cells in response to demyelination. Second, NgR blockade has a neuroprotective effect in demyelination condition. Yu and coworkers suggested that in addition to stimulating axon regeneration, NgR inhibition might also be neuroprotective, contributing to the overall functional recovery after spinal cord injury, which can be attributed to neuroprotective effect of NgR inhibition (Yu et al., 2008). Additional studies need to be carried out to clarify the molecular mechanisms by which NgR exerts its inhibitory effects on SVZ niche behaviors *in vivo*. Such research would contribute to therapeutic approach for successful repair in Multiple

Sclerosis.

Acknowledgments

The project was supported by Tarbiat Modares University. Work in B. Demeneix' laboratory is supported by the Association Francaise contre les Myopathies (AFM). Also the first author thanks Multiple Sclerosis International Federation (www.msif.org) for sabbatical support to complete this project.

Conflict of interest

The authors have declared that no competing interests exist.

References

Alvarez-Palazuelos LE, Robles-Cervantes MS, Castillo-Velazquez G, Rivas-Souza M, Guzman-Muniz J, Moy-Lopez N, et al. Regulation of neural stem cell in the human SVZ by trophic and morphogenic factors. Curr Signal Transduct Ther 2011; 6: 320-326.

Baer AS, Syed YA, Kang SU, Mitteregger D, Vig R, Ffrench-Constant C, et al. Myelin-mediated inhibition of oligodendrocyte precursor differentiation can be overcome by pharmacological modulation of FYN-RHOA and protein kinase C signalling. Brain 2009; 132: 465-481.

Chitnis T, Imitola J, Wang Y, Elyman W, Chawla P, Sharukh M, et al. Elevated neural expression of CD 200 protects wlds mice from inflammation-mediated neurodegeneration. Am J Pathol 2007; 170: 1695-1712.

Chong SY, Rosenberg SS, Fancy SP, Zhao C, Shen YA, Hahn AT, et al. Neurite outgrowth inhibitor Nogo-A establishes spatial segregation and extent of oligodendrocyte myelination. Proc Natl Acad Sci U S A. 2012; 109: 1299-1304.

Crespel A, Rigau V, Coubes P, Rousset MC, de Bock F, Okano H, Baldy-Moulinier M, Bockaert J, Lerner-Natoli M. Increased number of neural progenitors in human temporal lobe epilepsy. Neurobiol Dis 2005; 19: 436-450.

Curtis MA, Penney EB, Pearson AG, van Roon-Mom WM, Butterworth NJ, Dragunow M, et al. Increased cell proliferation and neurogenesis in the adult human Huntington's disease brain. Proc Natl Acad Sci U S A 2003; 100: 9023-2027.

Decherf S, Seugnet I, Kouidhi S, Lopez-Juarez A, Clerget-Froidevaux MS, Demeneix BA. Thyroid hormone exerts negative feedback on hypothalamic type 4 melanocortin receptor expression. Proc Natl Acad Sci U S A 2010; 107: 4471–4476.

Decker L, Picard-Riera N, Lachapelle F, Baron-Van Evercooren A. Growth factor treatment promotes mobilization young but not aged adult subventricular zone precursors in response to demyelination. J Neurosci Res 2002; 69: 763-771.

Dehghan S, Javan M, Pourabdolhossein F, Mirnajafi-Zadeh J, Baharvand H. Basic fibroblast growth factor potentiates myelin repair following induction of experimental demyelination in adult mouse optic chiasm and nerves. J Mol Neurosci 2012; 48: 77-85.

Fischer D, He Z, Benowitz LI. Counteracting the Nogo receptor enhances optic nerve regeneration if retinal ganglion cells are in an active growth state. J Neurosci 2004; 24: 1646-1651.

Fournier AE, GrandPre T, Strittmatter SM. Identification of a receptor mediating Nogo-66 inhibition of axonal regeneration. Nature 2001; 409: 341-346.

Fry EJ, Ho C, David S. A role for Nogo receptor in macrophage clearance from injured peripheral nerve. Neuron 2007; 53: 649-662.

Guazzo EP. A technique for producing demyelination of the rat optic nerves. J Clin Neurosci 2005; 12: 54-58.

Harvey PA, Lee DH, Qian F, Weinreb PH, Frank E. Blockade of Nogo receptor ligands promotes functional regeneration of sensory axons after dorsal root crush. J Neurosci 2009; 29: 6285-6295.

Huang JY, Wang YX, Gu WL, Fu SL, Li Y, Huang LD, et al. Expression and function of myelin-associated proteins and their common receptor NgR on oligodendrocyte progenitor cells. Brain res. 2012; 1437: 1-15.

Jin K, Peel AL, Mao XO, Xie L, Cottrell BA, Henshall DC, et al. Increased hippocampal neurogenesis in Alzheimer's disease. Proc Natl Acad Sci U S A 2004; 101: 343-347.

Karnezis T, Mandemakers W, McQualter JL, Zheng B, Ho PP, Jordan KA, et al. The neurite outgrowth inhibitor Nogo A is involved in autoimmune-mediated demyelination. Nat Neurosci 2004; 7: 736-744.

Kotter MR, Li WW, Zhao C, Franklin RJ. Myelin impairs CNS remyelination by inhibiting oligodendrocyte precursor cell differentiation. J Neurosci 2006; 26: 328-332.

Kremer D, Gottle P, Hartung HP, Kury P. Pushing forward: Remyelination as the new frontier in CNS diseases. Trends Neurosci 2016; 39: 246-263.

Li X, Su H, Fu QL, Guo J, Lee DH, So KF, et al. Soluble NgR fusion protein modulates the proliferation of neural progenitor cells via the notch pathway. Neurochem Res 2011; 36: 2363-2372.

Mathis C, Schro¨ter A, Thallmair M, Schwab ME. Nogo-A regulates neural precursor migration in the embryonic mouse cortex. Cereb Cortex 2010; 20: 2380-2390.

Mingorance A, Fontana X, Sole´ M, Burgaya F, Uren˜a JM, Teng FY, et al. Regulation of Nogo and Nogo receptor during the development of the entorhino-hippocampal pathway and after adult hippocampal lesions. Mol Cell Neurosci 2004; 26: 34-49.

Mohajeri M, Sadeghizadeh M, Najafi F, Javan M. Polymerized nano-curcumin attenuates neurological symptoms in EAE model of multiple sclerosis through down regulation of inflammatory and oxidative processes and enhancing neuroprotection and myelin

repair. Neuropharmacology 2015; 99: 156-167.

Mozafari S, Sherafat MA, Javan M, Mirnajafi-Zadeh J, Tiraihi T. Visual evoked potentials and MBP gene expression imply endogenous myelin repair in adult rat optic nerve and chiasm following local lysolecithin induced demyelination. Brain Res 2010; 1351: 50-56.

Mozafari S, Javan M, Sherafat MA, Mirnajafi-Zadeh J, Heibatollahi M, Pour-Beiranvand S, et al. Analysis of structural and molecular events associated with adult rat optic chiasm and nerves demyelination and remyelination: possible role for 3rd ventricle proliferating cells. Neuromolecular Med 2011; 13: 138-150.

Nait-Oumesmar B, Decker L, Lachapelle F, Avellana-Adalid V, Bachelin C, Baron-Van Evercooren A. Progenitor cells of the adult mouse subventricular zone proliferate, migrate and differentiate into oligodendrocytes after demyelination. Eur J Neurosci 1999; 11: 4357-4366.

Nait-Oumesmar B, Picard-Riera N, Kerninon C, Deccker L, Seilhean D, HÖlinger GU, et al. Activation of the subventricular zone in multiple sclerosis: Evidence for early glial progenitors. Proc Natl Acad Sci U S A 2007; 104: 4694-4699.

Noseworthy JH, Lucchinetti C, Rodriguez M, Weinshenker BG. Multiple sclerosis. N Engl J Med 2000; 343: 938-952.

Paxinos GF, Franklin KBJ. The mouse brain in stereotaxic coordinates. San Diego, California: Academic Press, 2004.

Pazhoohan S, Satarian L, Asghari AA, Salimi M, Kiani S, Mani AR, et al. Valproic Acid attenuates disease symptoms and increases endogenous myelin repair by recruiting neural stem cells and oligodendrocyte progenitors in experimental autoimmune encephalomyelitis. Neurodegener Dis 2014; 13: 45-52.

Petratos S, Ozturk E, Azari MF, Kenny R, Lee JY, Magee KA, et al. Limiting multiple sclerosis related axonopathy by blocking Nogo receptor and CRMP-2 phosphorylation. Brain 2012; 135: 1794-1818.

Picard-Riera N, Decker L, Delarasse C, Goude K, Nait-Oumesmar B, Liblau R, et al. Experimental autoimmune encephalomyelitis mobilizes neural progenitors from the subventricular zone to undergo oligodendrogenesis in adult mice. Proc Natl Acad Sci U S A 2002; 99: 13211-13216.

Picard-Riera N, Nait-Oumesmar B, Baron-Van Evercooren A. Endogenous adult neural stem cells: limits and potential to repair the injured central nervous system. J Neurosci Res 2004; 15; 76: 223-231.

Pourabdolhossein F, Mozafari S, Javan M, Mirnajafizadeh S J, Ahmadiani A. Electrophysiological and histological study of lysolecithin-induced local demyelination in adult mice optic chiasm. Physiol Pharmacol 2011; 14: 324-336.

Pourabdolhossein F, Mozafari S, Morvan-Dubois G, Mirnajafi-Zadeh J, Lopez-Juarez A, Pierre-Simons J, et al. Nogo receptor inhibition enhances functional recovery following lysolecithin-induced demyelination in mouse optic chiasm. PLoS One 2014; 9: e106378.

Pourabdolhossein F, Gil-Perotín S, Garcia-Belda P, Dauphin A, Mozafari S, Tepavcevic V, et al. Inflammatory demyelination induces ependymal modifications concomitant to activation of adult (SVZ) stem cell proliferation. Glia 2017; 65: 756-772.

Ramasamy S, Yu F, Hong Yu Y, Srivats H, Dawe GS, Ahmed S. NogoR1 and PirB signaling stimulates neural stem cell survival and proliferation. Stem Cells 2014; 32: 1636-1648.

Remaud S, Lopez-Juarez SA, Bolcato-Bellemin AL, Neuberg P, Stock F, Bonnet ME, et al. Inhibition of Sox2 expression in the adult neural stem cell niche in vivo by monocationic-based siR delivery. Mol Ther Nucleic acids 2013; 2: e89.

Rolando C, Parolisi R, Boda E, Schwab ME, Rossi F, Buffo A. Distinct roles of Nogo-A and Nogo receptor 1 in the homeostatic regulation of adult neural stem cell function and neuroblast migration. J Neurosci 2012; 32: 17788-17799.

Satoh J, Onoue H, Arima K, Yamamura T. Nogo-A and nogo receptor expression in demyelinating lesions of multiple sclerosis. J Neuropathol Exp Neurol 2005; 64: 129-138.

Sherafat MA, Javan M, Mozafari S, Mirnajafi-Zadeh J, Motamedi F. Castration attenuates myelin repair following lysolecithin induced demyelination in rat optic chiasm: an evaluation using visual evoked potential, marker genes expression and myelin staining. Neurochem Res 2011; 36: 1887-1895.

Sherafat MA, Heibatollahi M, Mongabadi S, Moradi F, Javan M, Ahmadiani A. Electromagnetic field stimulation potentiates endogenous myelin repair by recruiting subventricular neural stem cells in an experimental model of white matter demyelination. J Mol Neurosci 2012; 48: 144-53.

Steinbach K, McDonald CL, Reindl M, Schweigreiter R, Bandtlow C, Martin R. Nogo-receptors NgR1 and NgR2 do not mediate regulation of CD4 T helper responses and CNS repair in experimental autoimmune encephalomyelitis. PLoS One 2011; 6: e26341.

Su Z, Cao L, Zhu Y, Liu X, Huang Z, Huang A, et al. Nogo enhances the adhesion of olfactory ensheathing cells and inhibits their migration. J Cell Sci 2007; 120: 1877–1887.

Syed YA, Baer AS, Lubec G, Hoeger H, Widhalm G, Kotter MR. Inhibition of oligodendrocyte precursor cell differentiation by myelin-associated proteins. Neurosurg focus 2008; 24: E5.

Wang B, Xiao Z, Chen B, Han J, Gao Y, Zhang J, et al. Nogo-66 promotes the differentiation of neural progenitors into astroglial lineage cells through mTORSTAT3 pathway. PloS One 2008a: 3; e1856.

Wang F, Zhu Y. The interaction of Nogo-66 receptor with Nogo-p4 inhibits the neuronal differentiation of neural stem cells. Neuroscience 2008b; 151: 74-81.

Wang KC, Koprivica V, Kim JA, Sivasankaran R, Guo Y, Neve RL, et al. Oligodendrocyte-myelin glycoprotein is a Nogo receptor ligand that inhibits neurite outgrowth. Nature 2002a; 417: 941-944.

Wang T, Wang J, Yin C, Liu R, Zhang JH, Qin X. Down-

regulation of Nogo receptor promotes functional recovery by enhancing axonal connectivity after experimental stroke in rats. Brain Res 2010; 1360: 147-158.

Wang X, Chun SJ, Treloar H, Vartanian T, Greer CA, Strittmatter SM. Localization of Nogo-A and Nogo-66 Receptor proteins at sites of axonmyelin and synaptic contact. J Neurosci 2002b; 22: 5505-5515.

Yang Y, Liu Y, Wei P, Peng H, Winger R, Hussain RZ, et al. Silencing Nogo-A promotes functional recovery in demyelinating disease. Ann Neurol 2010; 67: 498-507.

Yu P, Huang L, Zou J, Yu Z, Wang Y, Wang X, et al. Immunization with recombinant Nogo-66 receptor (NgR) promotes axonal regeneration and recovery of function after spinal cord injury in rats. Neurobiol Dis 2008; 32: 535-542.